# Dynamics of kinks in smectic-*C* liquid crystals in periodically varying external fields

Sreejith Sukumaran* and G. S. Ranganath†
*Raman Research Institute, Sadashivanagar, Bangalore 560080, India*
(Received 14 February 1997)

We have considered the dynamics of kinks in smectic-*C* liquid crystal in uniformly rotating and oscillating electric or magnetic fields. In tilted oscillating fields our results are at variance with those of earlier investigations which predict chaos in this geometry for a $\pi$ kink. On the other hand, we find that the velocity and the structure of a $\pi$ kink are oscillatory with the frequency of the varying field. The average velocity as a function of the tilt angle of the field indicates a threshold angle beyond which there is a crossover in velocity selection with the system choosing from a family of solutions. Surprisingly, in a nonoscillating field rotating in a plane normal to the layers, a $\pi$ kink has a drift velocity whose direction is dependent upon the sense of rotation. As a result of this, a $2\pi$ kink could be in a bound oscillating state or it could split itself into two oppositely drifting oscillating $\pi$ kinks. In a nonoscillating tilted field rotating about the layer normal, in the synchronous regime we find an instability of a kink connecting a stable state and a metastable state. In the asynchronous regime, a kink connecting two stable states has aperiodic motion. Interestingly, in the same geometry in oscillating fields, we find that a kink joining a stable state and a metastable state is more stable. In this geometry, periodic and aperiodic fluctuating kink structures are also possible. We have suggested a simple way of understanding the general dynamical features of a kink on the basis of the dynamics of the uniform director state which is found to be very sensitive to parameters of the system. [S1063-651X(97)04408-5]

PACS number(s): 61.30.Cz, 61.30.Gd, 03.40.Kf, 75.60.Ch

## I. INTRODUCTION

Propagation of fronts or domain walls has been studied in analyses of reaction-diffusion equations and in physical models of different phenomena in fluid dynamics, dendritic growth, population growth, chemical reactions, and other biological models [1–12]. The nonlinear dynamics of liquid crystals under the action of external fields has invoked great theoretical and experimental interest in this subject [13–19]. In this context, it may be noted that ''solitons'' describing domain walls in liquid crystals are not solitons in the true sense. They are more in the nature of solitary waves. They do not have the essential characteristics of true solitons, namely, preservation of shape and momenta on a pairwise collision. This is a consequence of the fact that these are overdamped systems.

In this paper we discuss the dynamics of kinks in a smectic-*C* liquid crystal (Sm*C*) under the action of external fields. A kink is a permitted topological defect in an external electric or magnetic field. It is in the nature of a nonsingular wall connecting two uniform states. It is well known [13] that these start moving uniformly with a constant velocity when the potential energy becomes asymmetric. This could happen in two different ways. Either the uniform states themselves are at different potential energies, or the uniform states are at the same potential energy but the internal structure of the kink has an asymmetric potential energy. In the first case, the kink connects a stable state to a metastable state or an unstable state, while in the second case, the kink connects two stable states. We have considered the dynamical effects of varying, that is, oscillating and rotating, fields in these two cases.

A $\pi$ kink which has a topological winding of 180° moves uniformly with a constant velocity in a static field applied at an angle to the smectic layers. This motion is due to the potential difference between the uniform states. Schiller, Pelzl, and Demus [17] obtained an analytical solution which describes a uniformly moving $\pi$ kink. Recently, Sarloos, Hecke, and Holyst [16] solved a similar problem, and showed that, in a range of parameters, even though the nonlinear marginally stable analytical solution is valid, the system chooses a linear marginally stable solution with a different velocity. Such a crossover in velocity selection has been a topic of general interest in recent times [4,6–8,10,16]. Under a sudden destabilization, systems in a wide class of problems respond by forming a front which propagates from a stable to an unstable state or a metastable state. The problems of interest are whether the front evolves in time into a kink of a constant, unique speed, and, if so, how the system selects this speed from many possible speeds.

It is important to know what would happen when the field also has an oscillating component. In this context we must recall the work of Stewart, Carlsson, and Leslie [18,19]. They showed that in an oscillating tilted field, under certain assumptions, Melnikov analysis leads to chaotic instabilities in $\pi$ kinks. We have reconsidered this geometry in this paper, and our analysis leads to a nonchaotic behavior of these kinks. The structure and instantaneous velocity of the kink are found to be oscillatory at the frequency of the oscillating field. We find that an average velocity exists whose variation with the tilt of the field indicates a crossover in velocity selection as in the case of the nonoscillating field. In other words, the structure and velocity of a $\pi$ kink are not described by a single function of the tilt angle.

In a nonoscillating field rotating uniformly in a plane nor-

*Electronic address: sreesuku@rri.ernet.in
†Electronic address: gsr@rri.ernet.in

 

mal to the smectic layers, the potential energy varies periodically in time. Strangely, a kink develops a drift velocity over and above an oscillatory motion, and this drift is dependent on the direction of rotation. A consequence of this is that a $2\pi$ kink would either be in a bound oscillating state or split into oppositely drifting oscillating $\pi$ kinks depending upon the sense of rotation of the field.

In a static tilted field rotating about the layer normal, there exist two regimes [20]. Below a critical rotational frequency we have a synchronous regime in which the uniform state rotates with the rotating field with a constant phase lag, and above this frequency we obtain an asynchronous regime in which the uniform state rotates with phase slipping. This behavior of the uniform state is also very sensitive to the tilt angle of the field. Below a certain rotational frequency, as the tilt varies continuously from a direction parallel to the smectic layers to a direction normal to the layers, we find that if the system is already in the asynchronous regime it becomes synchronous at a critical tilt, and remains in that state till the tilt reaches a higher critical value at which it goes back to the asynchronous regime. This is reminiscent of reentrant behavior. Most theoretical studies to date are on kinks in the synchronous state, where a stable $\pi$ or $2\pi$ kink moves with a uniform velocity [14,15,21]. Not much attention has been paid to the dynamics of such kinks in the asynchronous regime. We find that the dynamics of the uniform state is helpful in the understanding of the dynamics of such a kink. In the asynchronous regime, the velocity and structure of the $2\pi$ kink becomes time dependent. The kink exhibits a translatory motion superimposed on an oscillatory motion. Further, due to the phase slipping of the uniform states in this regime, the dynamics is aperiodic, and a unique structure is not a permitted state.

In an oscillating field, rotating about the layer normal, the behavior of the uniform state is different. A time-averaged rotational frequency of the uniform state can be defined. The ratio of this rotational frequency to the frequency of the oscillating field is a rational number. Also, as the rotational frequency of the field is varied continuously, the time-averaged frequency of rotation of the uniform state varies in steps. On the basis of this behavior of the uniform state, we are able to predict qualitatively whether the dynamics of a $\pi$ or a $2\pi$ kink would be periodic or aperiodic.

Further, in this geometry, in a nonoscillating field the metastable state gradually drifts a little toward the stable orientation, and becomes unstable at a critical rotational frequency even before the onset of asynchronous motion. As a result, a $\pi$ kink gradually unwinds a little and becomes unstable against a uniform state at this frequency. Interestingly, in an oscillating field, these kinks are stabilized even when there is phase slipping, but have a time-dependent topological winding. Finally, we discuss the dynamics associated with a lattice of kinks, and find that the behavior of a single kink is sufficient to understand the behavior of the entire lattice.

## II. THEORY

Sm*C* liquid crystals are layered structures with the mean molecular alignment described by a director **n** tilted at an angle $\theta$ with respect to the layer normal **a**. We shall assume that the layers are of constant thickness. The projection of the director **n** onto the smectic planes is denoted by a unit vector **c** also called the **c** director. In an external electric or magnetic field, kinks or domain walls in the **c** vector field that do not disturb the layered structure are possible. They are either twist kinks, or splay-rich or bend-rich kinks. We shall be discussing the dynamics of only twist kinks in this paper since they need not be associated with backflow effects. In the case of splay-rich or bend-rich kinks, backflow effects would have to be considered. We use the continuum theory of Sm*C* as developed by Leslie, Stewart, and Nakagawa [19,22]. The free-energy density includes the elastic deformations of the **c** director and the energy density due to an applied external electric or magnetic field. In this paper we shall describe the effects of a magnetic field **H**. Incidentally, electric fields would produce similar results only if the material is free from ionic impurities.

In the Cartesian coordinate system, the layer normal is taken along the $z$ axis, that is, $\mathbf{a}=(0,0,1)$, and the director **n** is

$$\mathbf{n}=(\sin\theta\cos\phi,\sin\theta\sin\phi,\cos\theta),$$

where $\phi=\phi(z,t)$ is the angle that the **c** director makes with the $x$ axis. The free energy-density is

$$F=\frac{1}{2}\left[B_3\left(\frac{\partial\phi}{\partial z}\right)^2-\chi_a(\mathbf{n}\cdot\mathbf{H})^2\right], \tag{1}$$

where $B_3$ is the twist elastic constant and $\chi_a$ is the diamagnetic anisotropy of the Sm*C* in the local uniaxial approximation. The dynamical equation is given by

$$2\lambda_5\frac{\partial\phi}{\partial t}=-\frac{\delta F}{\delta\phi}, \tag{2}$$

where $\lambda_5$ is the twist viscosity coefficient. We consider a spatially homogeneous magnetic field described by

$$\mathbf{H}=H_0(a+b\cos\gamma t)(\cos\alpha\cos\omega t,\cos\alpha\sin\omega t,\sin\alpha), \tag{3}$$

where $\gamma$ is the angular frequency of the oscillating field, $\alpha$ is the angle that the field makes with the layers, and $\omega$ is the angular frequency of rotation about the layer normal, **a**. We discuss the dynamics of twist kinks in the three geometries depicted in Figs. 1(a), 1(b), and 1(c). In terms of the dimensionless quantities, $\tau=(\chi_a H_0^2/2\lambda_5)t$ and $\eta=\sqrt{\chi_a H_0^2/B_3}z$, the dynamical equation (2) can be written in the form

$$\begin{aligned}\frac{\partial\phi}{\partial\tau}=&\frac{\partial^2\phi}{\partial\eta^2}-(a+b\cos\gamma_0\tau)^2\\&\times[\sin\theta\cos\theta\sin\alpha\cos\alpha\sin(\phi-\omega_0\tau)\\&+\sin^2\theta\cos^2\alpha\sin(\phi-\omega_0\tau)\cos(\phi-\omega_0\tau)],\end{aligned} \tag{4}$$

where $\gamma_0=\gamma(t/\tau)$ and $\omega_0=\omega(t/\tau)$. In this paper, we have expressed time, distance, velocity and frequencies (of rotation and oscillation) with these dimensionless quantities. Hence $\tau=t/t_0$, $\eta=z/z_0$, $\omega_0=\omega t_0$, $\gamma_0=\gamma t_0$ and velocity (dimensionless) $=z_0/t_0$ velocity. The characteristic relaxation time and coherence length, $t_0$ and $z_0$ are $2\lambda_5/\chi_a H_0^2$ and

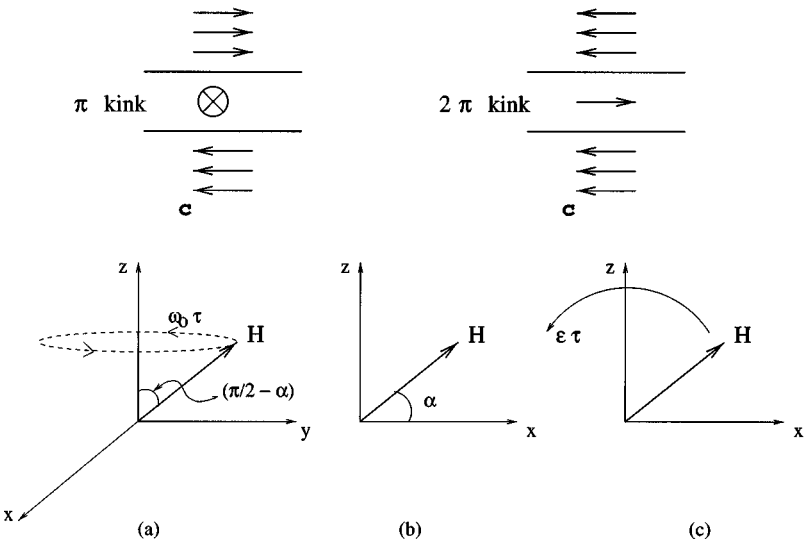


FIG. 1. Schematic representation of a $\pi$ kink, a $2\pi$ kink, and the three geometries in which the dynamics of a kink in an external magnetic field **H** are considered. (a) A field tilted at a constant angle $\alpha$ with respect to the layers rotating uniformly about the $z$ axis, the layer normal. (b) A nonrotating field at a constant tilt angle $\alpha$ with respect to the layers. (c) A constant field uniformly rotating in a plane $xz$, normal to the layers. In the representation of the kinks, the arrows indicate the direction of the **c** vector. Inside the kink, it turns (about the $z$ axis, the direction of the smectic layer normal) through $\pi$ or $2\pi$.

$\sqrt{B_3/\chi_a H_0^2}$, respectively. Since our results are independent of the phase of the oscillating field, we shall take it to be zero.

This is an overdamped double sine-Gordon equation, and it is applicable to systems other than Sm*C*. When $\alpha=0$, Eq. (4) reduces to the normal sine-Gordon equation describing nematics in an external field. When $\alpha\neq 0$, it can be used to describe field effects in ferronematics which are usual nematics with doped ferromagnetic grains. A variant of Eq. (4) can describe front propagation in chiral smectic liquid crystals [16].

We have numerically solved this partial differential equation by the method of lines using Numerical Algorithms Group (NAG) Fortran Library subroutines to study the dynamics of kinks. We look for kink solutions which necessitate the boundary condition, $[\partial\phi/\partial\eta]_{\eta=\pm L}=0$, where $L$ is the extent of the system in dimensionless units. We have taken $L=1000$ with a mesh size $\delta L=0.1$. We first excite a discontinuous twist in the homogeneous state. This is equivalent to, numerically, a step function in distortion. Then we study its time evolution to a stable form. For example, to create a propagating $2\pi$ kink, it is sufficient to have a step of $2\pi$ at the origin as the initial profile. The shape of the profile does not alter the asymptotic or late-time results as long as the net amplitude is large enough.

## III. RESULTS

As mentioned above, kinks can start moving when the potential energy in the external field becomes asymmetric. An understanding of the dynamical behavior of the uniform state helps us considerably in predicting the essential dynamical features of kinks. Hence we first discuss the dynamics of the uniform state. Afterwards we consider the effects of a periodically varying magnetic field on kinks connecting a stable state to a metastable state or an unstable state and kinks connecting stable states. In the first case, we shall deal with a $\pi$ kink in various geometries and in the latter case, a $2\pi$ kink will be the chosen representative.

### A. Uniform state

In the case of an uniform state, the azimuthal angle $u=(\phi-\omega_0\tau)$ between the director and the field obeys the ordinary differential equation

$$\frac{du}{d\tau}=-\omega_0-(a+b\cos\gamma_0\tau)^2[\sin\theta\cos\theta\sin\alpha\cos\alpha\sin u+\sin^2\theta\cos^2\alpha\sin u\cos u]. \quad (5)$$

In a nonoscillating field ($\gamma_0=0$) with $\alpha=0$, Eq. (5) yields analytical solutions, but, with $\alpha\neq 0$, the analytical solution is a complicated function. Numerical integration with a fourth-order Runge-Kutta method reveals that the general features are nearly the same in both these cases. The major difference is that in the case of $\alpha\neq 0$, the symmetry of the system makes the states $u$ and $(u+2\pi)$ equivalent with regard to their potential energy, while, in the case of $\alpha=0$, the states $u$ and $(u+\pi)$ are equivalent. In a steady state, the behavior of the system falls in two regimes [20]: (i) the *synchronous* regime, where the director follows the field with an angle constant in time; and (ii) the *asynchronous* regime, where there is slip between the field and the director. These two regimes are demarcated by a critial rotational frequency of the field, $\omega_0=\omega_c$. In Fig. 2, we show the dependence of $\omega_c$ on $\alpha$ for a given $\theta$. Interestingly, at an $\omega_0$ below a threshold, as the tilt angle $\alpha$ increases from zero, we find a transition from an asynchronous to a synchronous state and at a still higher $\alpha$ a transition back to an asynchronous state. This reentrant behavior is characteristic of Sm*C*.

In a tilted nonrotating field, $\phi=0$ is always a stable state, and in addition we also find a metastable state at $\phi=\pi$ exists for $\alpha<\alpha_c$, a critical value of the tilt. When a field at $\alpha<\alpha_c$ rotates about the layer normal, the relative orientation of both these states changes. The stable state shows a monotonic variation. However, the metastable state gradually shifts toward the stable state, that is, lower values of $\phi$, till at a critical rotational frequency it switches to the stable state. This critical frequency is less than the critical frequency at which asynchronous regime sets in. Figure 3 shows these features.

In the asynchronous regime, the uniform stable state follows the field with an angle which is a nonlinear function of time. At a given rotational frequency of the field, the uniform state changes its orientation as depicted in Fig. 4. For long intervals of time, the uniform state remains nearly unperturbed but, at regular intervals, it suffers a ''stick-slip'' lead-

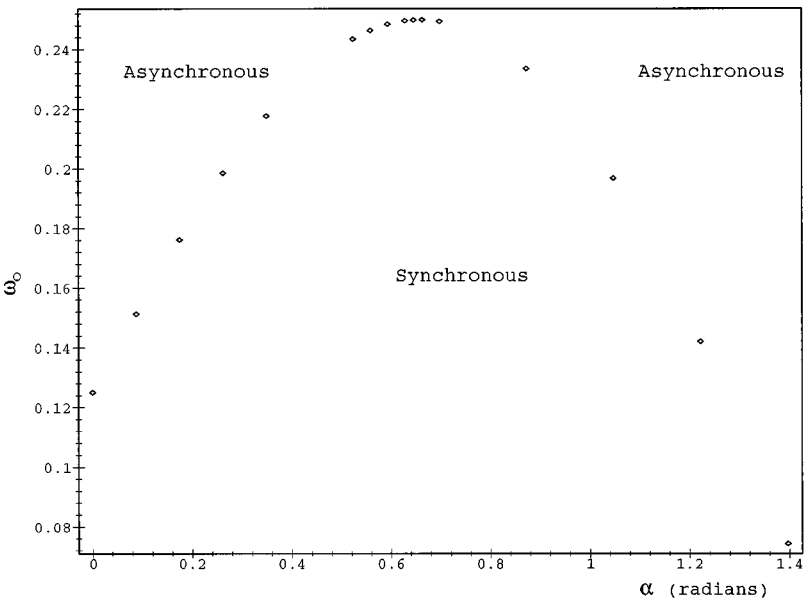


FIG. 2. $\omega_0$-$\alpha$ diagram depicting the asynchronous to synchronous transition in a constant field in the geometry shown in Fig. 1(a). Below a threshold rotational frequency, asynchronous to synchronous and back to asynchronous transitions are seen as $\alpha$ varies from 0 to $\pi/2$ rad. Here $a=1$, and $b=0$.

ing to a phase slip of $2\pi$ for $\alpha\neq 0$; for $\alpha=0$, this phase slip is $\pi$. This interval is a continuous function of $\omega_0$.

With an oscillating rotating field, we find that the dynamics of the uniform state is very different from what we obtained in a nonoscillating rotating field. In an oscillating field, we have a regime very similar to the synchronous regime; here we have the **c** director following the field oscillating about a fixed direction relative to the field. These oscillations are at the frequency of the oscillating field. We call this the *phase-oscillating* regime. The relative mean orientation of the director with respect to the field direction gradually increases as $\omega_0$ increases. Above a critical value of the rotational frequency, $\omega_c'$, the behavior of the uniform state is rather similar to the already described asynchronous regime in that there exists a phase slip. We call this the *phase-slipping* regime. In the case of the asynchronous regime in a nonoscillating field, there is a frequency for phase slip to an equivalent state which varies continuously as one varies the rotational frequency. However, with an oscillating field, this is not the case. We find that the uniform state always responds in such a way that in $n$ cycles of the oscillating field, the uniform state would have rotated, in the frame of reference of the rotating field, by $2\pi m$ (or $\pi m$) for $\alpha\neq 0$ (or $\alpha=0$). In this case, we can define the *phase-slip frequency* $w$ as

$$w=\frac{u(\tau+nT)-u(\tau)}{nT}=\frac{2\pi m}{nT}, \tag{6}$$

where $T$ is the period of the oscillating field. (We may recall here that Jung, Kissner, and Hänggi [23] described the motion of an overdamped particle in an asymmetric ''ratchet'' potential in a similar way.) Incidentally, $w=0$ for the phase-oscillating regime. Our numerical analysis indicates that $w$ is always a rational fraction of the frequency, $\gamma_0$, of the oscillating field with $w$ varying with the rotational frequency, $\omega_0$, as shown in Fig. 5. In Table I we give the values of $m$ and $n$ for different values of $\omega_0$. This clearly shows the extreme sensitivity of $m$ and $n$ to values of $\omega_0$. The essential features for any $\alpha$, $\gamma_0$, $a$, $b$, and $\theta$ are (i) the steplike behavior and; (ii) the fact that, for large $\gamma_0$, $w$ varies nearly linearly with $\omega_0$ and the length of steps, if present, is too

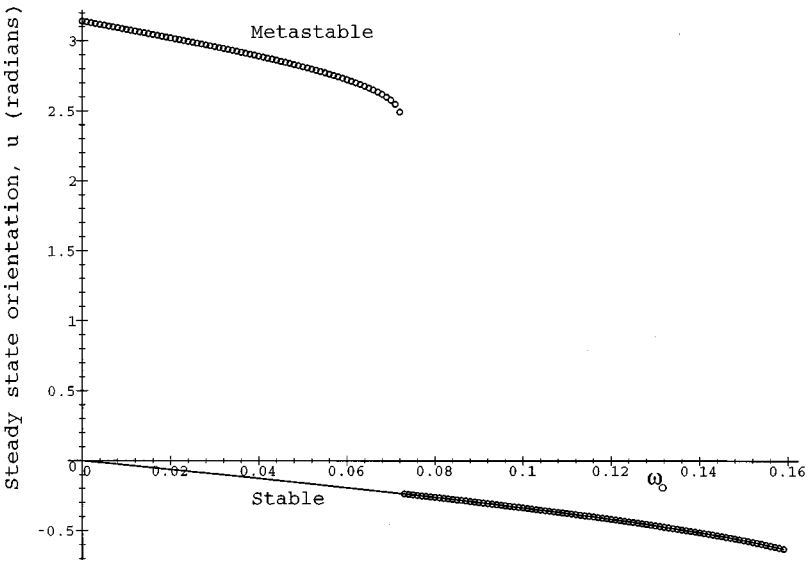


FIG. 3. The variation of the steady-state angle $u$ (of a uniformly oriented sample [Fig. 1(a)]) between **c** and **H** with rotational frequency. The circles and continuous line correspond to the initial metastable $u(\tau=0)=\pi$ and stable $u(\tau=0)=0$ states, respectively. The metastable state becomes unstable and collapses to the stable state at a critical rotational frequency. Here $\alpha=10°$ and $\theta=\pi/6$ rad.

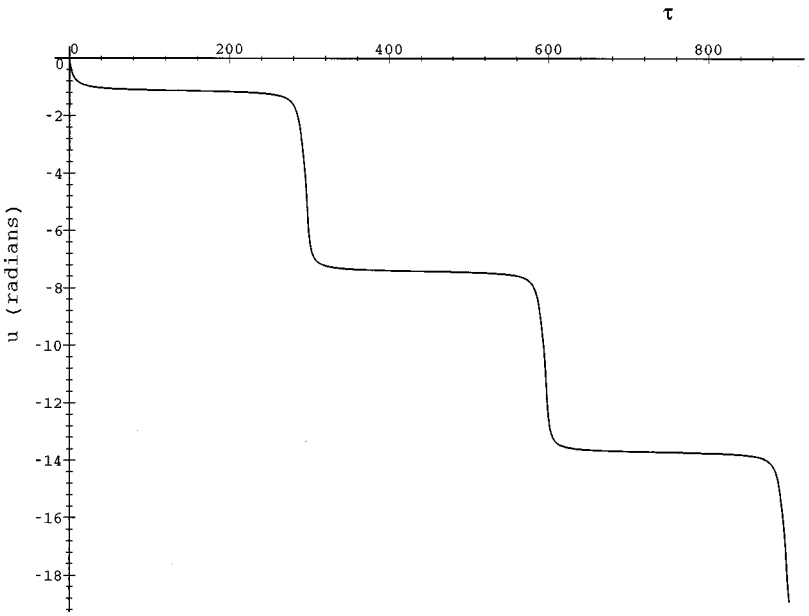


FIG. 4. Variation of the angle $u$ between **c** and **H** as a function of time in the asynchronous regime [Fig. 1(a)]. We find a sudden jump by $2\pi$ at regular intervals. Here $a=1$, $b=0$, $\omega_0=0.25$, and $\alpha=40°$.

small to show any departure from linearity. It should be noted that the integers $m$ and $n$ are dependent on the parameters of the problem.

### B. Kinks connecting a stable state to a metastable state or an unstable state

#### *1. Tilted nonrotating nonoscillating field*

In this case [see Fig. 1(b)], $\gamma_0=\omega_0=0$. Equation (4) permits a uniformly moving $\pi$ kink, described by [17]

$$\phi=2\tan^{-1}\exp[(\eta-\cos\theta\,\sin\alpha\tau)\sin\theta\,\cos\alpha]. \tag{7}$$

The velocity $v$ of the propagating kink is

$$v=\cos\theta\,\sin\alpha \tag{8}$$

It was recently shown by Sarloos, Hecke, and Holyst [16] that there can exist two different regimes, which are referred to as linear and nonlinear marginal-stability regimes. In the linear marginal-stability regime, the front speed can be calculated explicitly from perturbation analysis at the leading edge of the front. The deviations from the unstable state are small, and one can obtain the dispersion equation from the linearized equations. The velocity obtained from such a linear marginal-stability analysis, $v_l$, is given by

$$v_l=2\sqrt{\sin\theta\,\cos\theta\,\sin\alpha\cos\alpha-\sin^2\theta\cos^2\alpha}\,. \tag{9}$$

In the nonlinear marginal-stability regime the front speed depends on the fully nonlinear behavior of the equation. Here, they show that Eq. (8) corresponds to the nonlinear marginal-stability regime. Equations (8) and (9) are valid for $0\leqslant\alpha\leqslant\pi/2$. Similar solutions exist for other values of $\alpha$. These authors conjecture that there exists multiple stable traveling-wave solutions satisfying the dynamical equation, but the system chooses that particular solution which has the fastest spatial decay at the leading edge of the front. It is

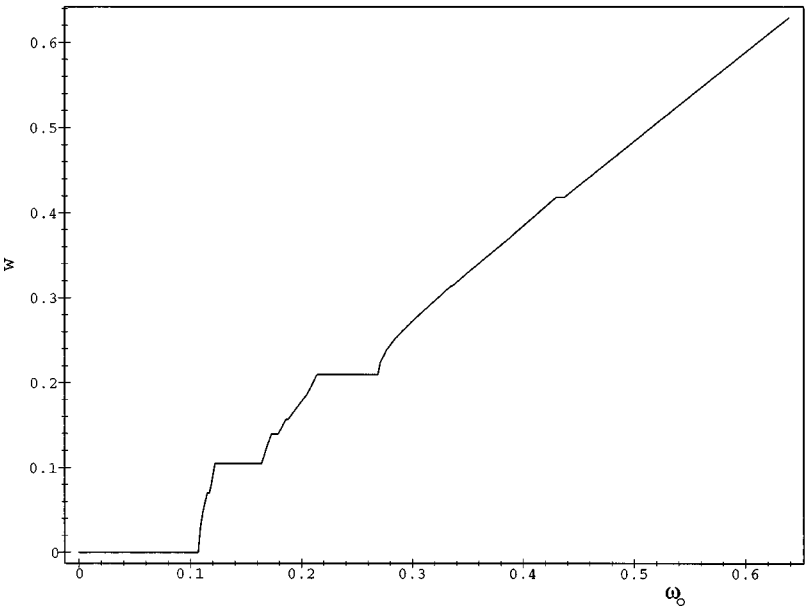


FIG. 5. The *phase-slip frequency* $w$ as a function of the rotational frequency of the field $\omega_0$. Below a critical $\omega_0=\omega_c'$ we find only the phase-oscillating regime. Here, $a=0.8$, $b=0.3$, $\gamma_0=2\pi/30$, $\alpha=10°$, and $\theta=\pi/6$ rad.

TABLE I. The values of $m$ and $n$ of $w$ for different $\omega_0$. They are very sensitive to values of $\omega_0$. The fixed parameters are $a=0.8$, $b=0.3$, $\theta=\pi/6$ rad, $\alpha=10°$, and $\gamma=2\pi/30$.

| $\omega_0$ | $m$ | $n$ | $\omega_0$ | $m$ | $n$ |
|---|---|---|---|---|---|
| $0\rightarrow0.107$ | 0 | 1 | 0.271 | 63 | 59 |
| 0.109 | 1 | 7 | 0.277 | 305 | 267 |
| 0.111 | 2 | 9 | 0.284 | 169 | 141 |
| 0.112 | 1 | 4 | 0.291 593 59 | 5 | 4 |
| $0.115\rightarrow0.117$ | 1 | 3 | 0.299 715 606 | 13 | 10 |
| 0.119 | 311 | 800 | 0.305 363 042 | 4 | 3 |
| $0.122\rightarrow0.164$ | 1 | 2 | $0.335\rightarrow0.336$ | 3 | 2 |
| 0.169 | 3 | 5 | 0.349 301 85 | 11 | 7 |
| $0.173\rightarrow0.179$ | 2 | 3 | 0.367 657 157 | 5 | 3 |
| $0.186\rightarrow0.188$ | 3 | 4 | 0.368 | 337 | 202 |
| 0.194 | 4 | 5 | 0.383 959 62 | 7 | 4 |
| 0.198 | 5 | 6 | $0.430\rightarrow0.437$ | 2 | 1 |
| 0.201 | 6 | 7 | 0.438 | 549 | 274 |
| 0.205 | 8 | 9 | 0.637 | 665 | 222 |
| $0.214\rightarrow0.269$ | 1 | 1 | 0.638 | 3 | 1 |

such a crossover in velocity selection that has been the topic of discussion in recent times. The interest has been in equations of the type

$$\frac{\partial\beta}{\partial t}=F_1(\beta_{zz},\ldots)+F_2(\beta), \tag{10}$$

where $F_1$ is a linear function of the spatial derivatives of $\beta$, and $F_2$ is a nonlinear function of $\beta$. We shall not discuss the various conjectures put forward to explain the phenomenon of velocity selection. In Fig. 6, we show the dependence of the velocity of a $\pi$ kink on $\alpha$, for $\theta=30°$ as given by Eqs. (8) and (9). We have also given our numerical results obtained by studying the evolution of a step for the sake of comparison. It should be noted that the curves for velocity $v_l$ in the linear marginal-stability regime, and the velocity $v$ in the nonlinear marginal-stability regime, are mutually tangential to one another at the crossover point, which is obtained from the relation

$$\cot\theta\tan\alpha=2. \tag{11}$$

It should be noted that such a crossover in velocity selection has been predicted only in cases where an analytical solution could be obtained.

#### *2. Tilted nonrotating oscillating field*

In this case of $\omega_0=0$ and $\gamma_0\neq0$, Stewart, Carlsson, and Leslie [18,19] concluded that for a weak slowly oscillating field at a small tilt, the dynamics of a $\pi$ kink exhibits chaos for certain ranges of the parameters. Their analysis assumes the existence of a uniform moving frame in which the dynamical equations reduce to a system of ordinary differential equations.

We have reconsidered the behavior of a $\pi$ kink in the same geometry. The range of different parameters is $2\pi/2048\leqslant\gamma_0\leqslant2\pi$, $0°\leqslant\alpha\leqslant85°$, $10°\leqslant\theta\leqslant80°$, $0\leqslant a\leqslant1$, $0\leqslant b\leqslant1$. We have also considered the domain of parameters, *viz.* $a=1$, $b=0.1$, $\theta=30°$, $\alpha=5°$, and $\gamma_0=\pi/150$, $\pi/125$, and $\pi/100$, in which Stewart, Carlsson, and Leslie predicted chaos.

We are interested in the long-time or asymptotic features in the dynamics of a $\pi$ kink. To characterize the dynamics of the entire kink, we followed the time evolution of three ''marked'' states, of the **c** director, in the $\pi$ kink. They are at $\phi=\pi/4$, $\pi/2$, and $3\pi/4$ . The distance between $\phi=\pi/4$ and $3\pi/4$ is a measure of the width of the kink. In Fig. 7, we give the time evolution of the three ''marked'' states. We find the instantaneous velocity at any point of the kink and the kink width to be periodic in time in all the cases we considered. The motion is asymmetric in space, since the three ''marked'' states behave differently. The frequency of the kink's structural pulsations and that of the velocity modulation of the ''marked'' states are equal to the frequency of the oscillating field when $a\neq0$, and twice it when $a=0$. Figure 8 shows six ''snapshots'' of the motion of the entire kink. It

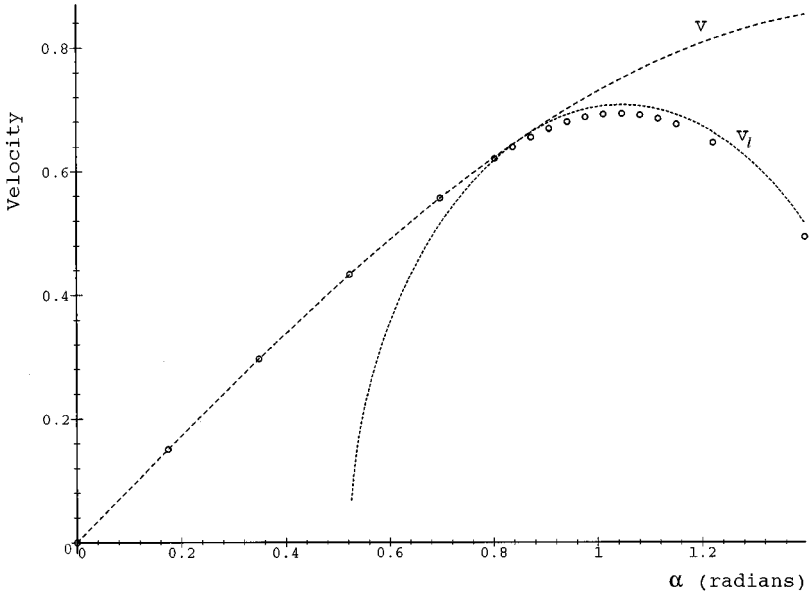


FIG. 6. Velocity of a $\pi$ kink as a function of the tilt, $\alpha$, of the field. Long dashed curve corresponds to the velocity $v$ in the nonlinear marginal stability regime and the short dashed curve corresponds to the velocity $v_l$ in the linear marginal stability regime. The circles are obtained from the numerical solution of Eq. (4). Here $\theta=\pi/6$ rad.

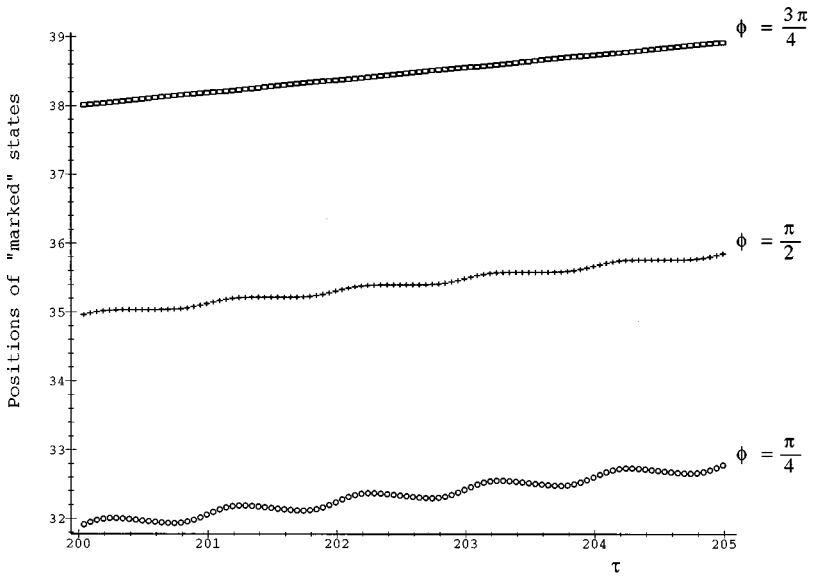


FIG. 7. Time evolution of the ''marked'' states, $\phi=\pi/4$ ($\bigcirc$), $\pi/2$ ($+$), and $3\pi/4$ ($\square$), of a $\pi$ kink in a tilted oscillating field [Fig. 1(b)]. Here $a=b=0.5$, $\alpha=20°$, $\gamma_0=2\pi$, and $\theta=\pi/6$ rad.

depicts all the above-mentioned features.

In an oscillating field, too, it is relevant to know whether there is a crossover in velocity selection due to the system choosing from families of solutions. There is no simple way of obtaining an analytical solution. Further, methods employed in the linear marginal-stability analysis do not work, since perturbations at the leading edge of the front should have time-dependent frequency and spatial decay. As a first attempt in understanding this problem, we inspect the variation of a time-averaged kink velocity with the tilt angle $\alpha$.

In view of the periodicity in the dynamics of a $\pi$ kink, we define an *average velocity* $v_a$ for every state $\phi_i$ at $\eta_i$ on the kink as

$$v_a=\frac{\eta_i(\tau+T)-\eta_i(\tau)}{T}. \tag{12}$$

Since the kink pulsates with the frequency, $\gamma_0=2\pi/T$, $v_a$ is unique for the entire kink. In Fig. 9, we show the dependence of $v_a$ on $\gamma_0$ at fixed values of $a$, $b$, $\theta$, and $\alpha$. A question of relevance at this point is whether $v_a$ approaches the ''dc limit'' as one goes to the limit $\gamma_0\to 0$. At $\gamma_0=0$, our time-averaged velocity is certainly an ill-defined quantity, and, hence, such a limit is not meaningful. This is analogous to the behavior of a charged particle in an oscillating field where the average velocity is zero for any finite frequency. Such an average does not go to the limit of nonzero velocity when the frequency goes to zero. The breakdown of the defined average velocity can be ascribed to the fact that the dc limit is a bifurcation point separating periodic behavior from nonperiodic behavior. We find that $v_a$ quickly approaches a fixed asymptotic value $v_r$, which we call the *root-mean-square* or *rms velocity*. It can be seen that $v_a$ is nearly $v_r$ at $\gamma_0\sim 2\pi$. In all the cases considered by us, we have found that this velocity is given by either of the two following equations:

$$v_r'=\left(a^2+\frac{b^2}{2}\right)^{1/2}\cos\theta\sin\alpha \tag{13}$$

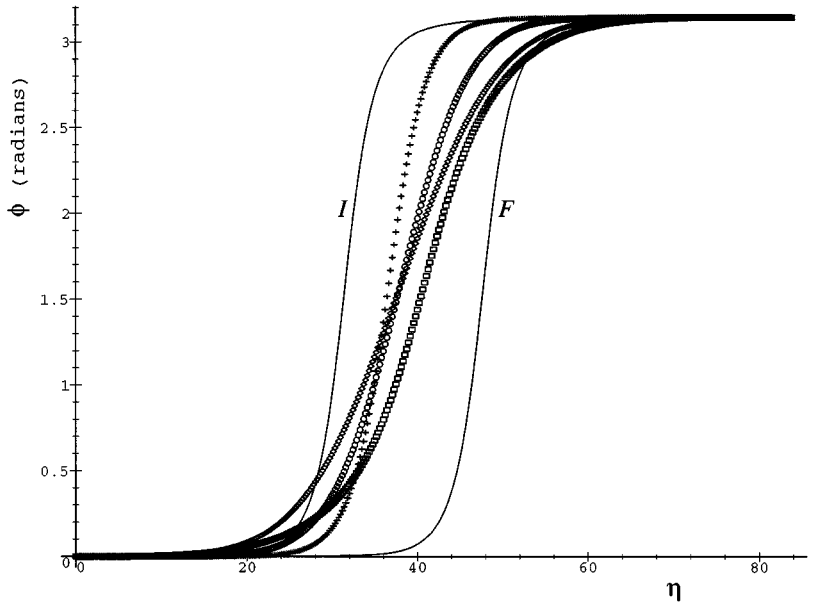


FIG. 8. ''Snapshots'' of a $\pi$ kink at different times $\tau=200$ (I), 220 ($+$), 240 ($\bigcirc$), 260 ($\diamond$), 280 ($\square$), and 300 ($F$). Here $a=b=0.5$, $\alpha=20°$, $\gamma_0=2\pi/100$, and $\theta=\pi/6$ rad.

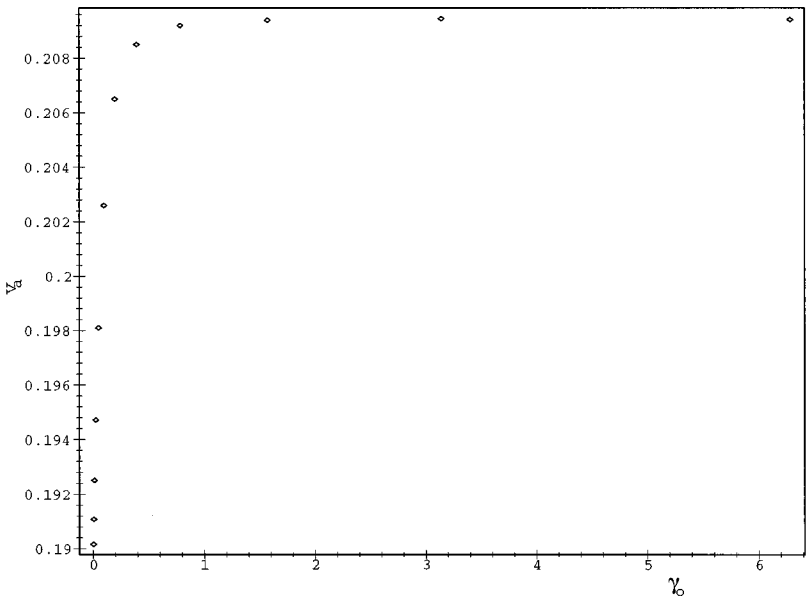


FIG. 9. Average velocity of a $\pi$ kink as a function of frequency, $\gamma_0$ of oscillating field [Fig. 1(b)]. Here, $a=0$, $b=1$, $\alpha=20°$, $\theta=\pi/6$ rad.

or

$$v_r'=2\left(a^2+\frac{b^2}{2}\right)^{1/2}\sqrt{\sin\theta\cos\theta\sin\alpha\cos\alpha-\sin^2\theta\cos^2\alpha}. \tag{14}$$

These are akin to Eqs. (8) and (9). In Fig. 10, we show $v_a$ versus $\alpha$ for $\gamma_0=2\pi$ for values of $a$, $b$, and $\theta$. It can be seen that there is a close agreement between the numerically calculated points and the analytical curves. This can be taken as an indication that in the case of oscillating fields also, there is a crossover in velocity selection. In this case, too, the system seems to be choosing an unique solution from families of solutions. As in the analysis of Sarloos, Hecke, and Holyst [16], here also the numerically computed velocities are slightly below the ones predicted by Eq. (14) in the linear marginal stability regime, and this is possibly due to slow convergence to the asymptotic value in this regime. For other values of $\gamma_0$ also, $v_a$ has a similar dependence on $\alpha$, but we could not fit an analytical function.

Our analysis raises an important question about the velocity selection in systems more general than that described by Eq. (10). Our results indicate that this phenomenon might occur in a broader class of physical systems obeying

$$\frac{\partial\beta}{\partial t}=G_1(\beta_{zz},\ldots)+G_2(t,\beta), \tag{15}$$

where $G_1$ is a linear function of the spatial derivatives of $\beta$, and $G_2$ is a nonlinear function of $\beta$ and *time also*. To our knowledge, this is the first indication of a system choosing between families of fronts which are not uniformly traveling, that is, $\beta(z,t)=U(z-ct)$, but varying periodically in time. The recent work of Armero *et al.* [24] considered the effects of external noise in a one-dimensional model of front propagation is an example of a system described by Eq. (15).

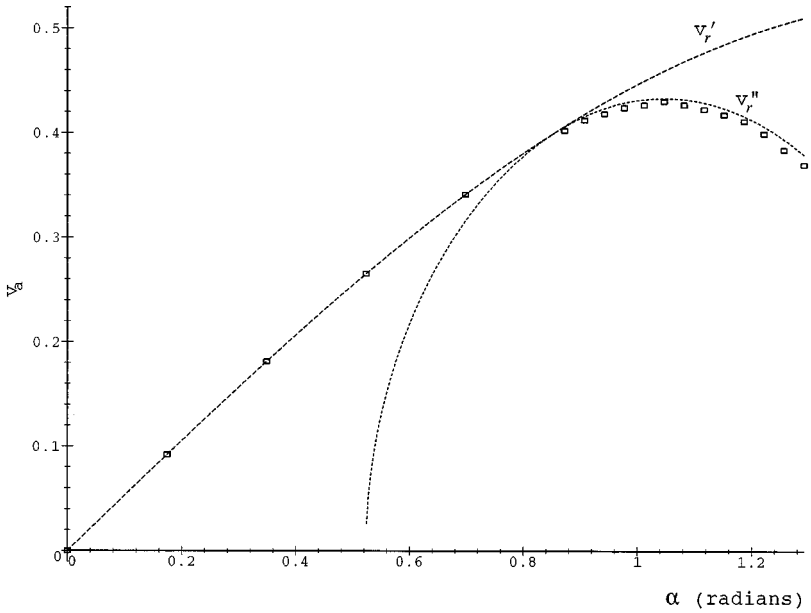


FIG. 10. Average velocity of a $\pi$ kink as a function of the tilt $\alpha$ in an oscillating field [Fig. 1(b)]. The long dashed curve corresponds to $v_r'$, and the short dashed curve corresponds to $v_r''$. The boxes are from the numerical solution of Eq. (4). The numerical results agree with $v_r'$ below the threshold tilt angle given by Eq. (11) and above that it agrees with $v_r''$. Here $a=b=0.5$, $\gamma_0=2\pi$, and $\theta=\pi/6$ rad.

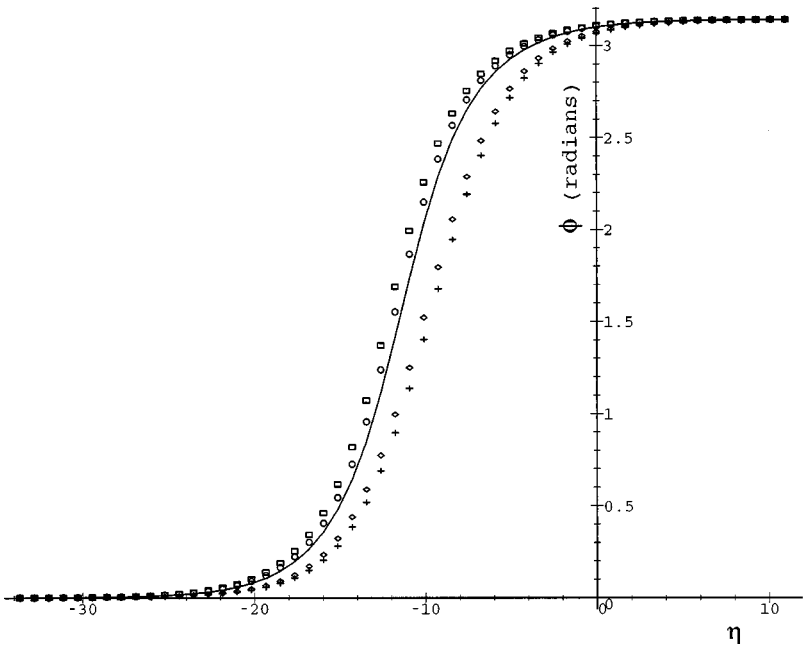


FIG. 11. ''Snapshots'' of a $\pi$ kink in a field uniformly rotating in the anticlockwise direction. [Fig. 1(c)]. The snapshots are at the times $\tau=300$ (-), 305 (+), 310 (○), 315 (◇), and 320 (□). The $\pi$ kink fluctuates periodically with a frequency of $2\pi/10$. The kink drifts such that the state $\phi=\pi$ expands at the expense of the state $\phi=0$. For clockwise rotation, the drift is such that the state $\phi=0$ expands at the expense of the state $\phi=\pi$. Here $a=1$, $b=0$, $\alpha=\epsilon\tau$, $\epsilon=2\pi/20$, and $\theta=\pi/6$ rad.

#### *3. Nonoscillating field rotating in a plane normal to the layers*

Here [see Fig. 1(c)] we have $b=0$, $\omega_0=0$, and $\alpha=\epsilon\tau$, where $\epsilon$ is the rotational frequency of the field. We find that the structure and velocity of a $\pi$ kink oscillates with a frequency equal to $2\epsilon$. But the surprising result is that there is an average drift velocity for the kink. In Fig. 11, ''snapshots'' of the motion of a $\pi$ kink are shown. Since Eq. (4) is invariant under the transformation $\phi\rightarrow(\pi-\phi)$, $\epsilon\rightarrow-\epsilon$, we know that the drift would be in the opposite direction if the direction of rotation of the field is reversed. We do find that for an anticlockwise rotation, i.e., $\epsilon>0$, the kink propagates such that the state $\phi=\pi$ expands at the expense of the state $\phi=0$. For a clockwise rotation, i.e., $\epsilon<0$, it is the state $\phi=0$ that expands at the expense of the state $\phi=\pi$. We also find that the drift velocity of the kink tends to zero as $\epsilon$ increases.

#### *4. Tilted field rotating about the layer normal*

We found in Sec. III A that in this geometry [see Fig. 1(a)], the uniform metastable state drifts toward the stable state as the frequency of the rotation increases. But, at a critical value of the rotational frequency, $\omega_c'$, it collapses to the stable state. This result helps us to understand the dynamics of a kink connecting a stable state to a metastable state as obtained by solving Eq. (4). These structures are simulated by the evolution of an initial step of height $\pi$. Referring to Fig. 3, we can say that these structures can exist with nearly the same topological winding of $\pi$ up to a rotational frequency $\omega_c'$ at which it suddenly becomes unstable and unwinds into an uniform state since the metastable state becomes unstable. Interestingly, in an oscillating field, the $\pi$ kink is not ironed out to the uniform state even in the phase-slipping regime. But the nonintegral topological winding number becomes time dependent.

### C. Kinks connecting stable states

In this section, we bring out the dynamical effects of a periodically varying magnetic field on a $2\pi$ kink. It should be noted that the results can be extended to the case of a $\pi$ kink when $\alpha=0$.

#### *1. Tilted nonrotating oscillating field*

We studied the effects of a tilted nonrotating oscillating field, [see Fig. 1(c)], on a $2\pi$ kink. The kink is stationary, as is to be expected from pure symmetry considerations, since the base states are at the same potential energy and the potential energy is symmetric about the center of the kink. The structure changes periodically with time. The variations are symmetric about the center. The state $\phi=\pi$ is stationary, and the average velocity of any other state is also zero.

#### *2. Nonoscillating field rotating in a plane normal to the layers*

At any given $\alpha$, a $2\pi$ kink is a permitted static solution when the field is nonrotating and nonoscillating. We considered the stability of a $2\pi$ kink in the geometry of Fig. 1(c). A $2\pi$ kink always splits when $\phi=\pi$ becomes a metastable state. In view of what has been said earlier, for clockwise rotation, the individual pulsating $\pi$ kinks drift toward one another. Hence we end up with a bound oscillating $2\pi$ kink state. On the other hand, for anticlockwise rotation, the individual pulsating $\pi$ kinks drift apart leading to a complete splitting of the $2\pi$ kink state. These are depicted in Figs. 12(a) and 12(b).

#### *3. Nonoscillating field rotating about the layer normal*

Figure 1(a) describes the geometry under discussion. In this case, we find the following results.

*Synchronous regime:* In the synchronous regime the potential difference between the two base states of a kink is a constant, and a uniformly moving kink exists. Büttiker and Landauer [21] showed that the kink velocity monotonically increases as the rotational frequency $\omega_0$ tends to the critical value $\omega_c$ at which asynchronous motion sets in. In Fig. 13, we show a variation of the kink velocity with $\alpha$ for a given $\theta$ and for three different values of $\omega_0$. The kink velocity goes through a minima as $\alpha$ is increased. Our data have been given only up to the onset of the asynchronous regime. It is known that the direction of kink propagation is dictated *only* by the sense of rotation of the external field.

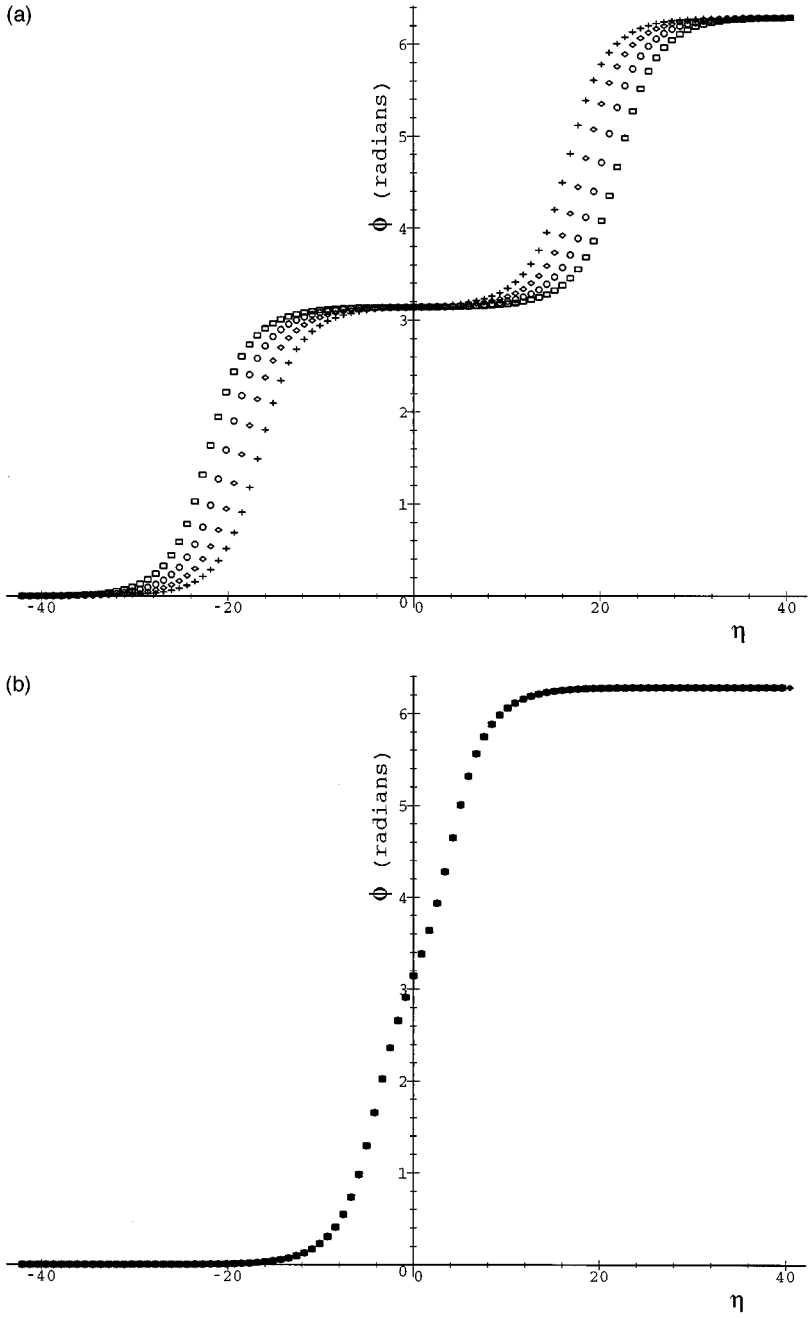


FIG. 12. ''Snapshots'' of the motion of a $2\pi$ kink in a field rotating [Fig. 1(c)], at $\tau=300$ (+), 350 ($\diamond$), 400 ($\bigcirc$), and 450 ($\square$). (a) Anticockwise rotation with $\epsilon=2\pi/20$ leads to a splitting of a $2\pi$ kink. (b) Clockwise rotation with $\epsilon=-2\pi/20$ leads to a bound $2\pi$ kink state. Here $a=1$, $b=0$, $\alpha=\epsilon\tau$, and $\theta=\pi/6$ rad.

*Asynchronous regime:* We already described the dynamical behavior of the uniform state in the asynchronous regime. There is a time scale over which the variation of $u$ is small, and then $u$ experiences a ''stick-slip'' over a short interval of time as depicted in Fig. 4. Due to this, the structure of the kink becomes time dependent. One can expect a nearly uniformly moving kink during the time in which the angle made by the uniform state with the field is hardly perturbed. In the time interval in which the uniform state experiences the stick-slip, kink features like width and velocity can be expected to change rapidly. Thus the structure of the $2\pi$ kink would have an oscillatory motion superimposed on a translatory motion. These features are depicted in Fig. 14, which shows the time evolution of the three ''marked'' positions $[u(\eta)-u(-\infty)]=\pi/2$, $\pi$, and $3\pi/2$ of the kink. Within the range of our numerical investigation, we can conclude, qualitatively, that a $2\pi$ kink in the asynchronous regime has the following features:

(i) On long-time scales, the center of the kink at $[u(\eta)-u(-\infty)]=\pi$ drifts in either direction.

(ii) Even on a time scale of $T\simeq 5000$, i.e., the asymptotic or long-time limit, the kink does not seem to have a uniform velocity or width. Due to the effects of a natural finite relaxation time of the director and because of the rapid variation due to the stick-slip, the width and velocity are aperiodic in time.

#### *4. Oscillating field rotating about the layer normal*

We have seen that the dynamics of the uniform state in this geometry [see Fig. 1(a)], is characterized by the pair of numbers $(m,n)$ describing the phase-slip frequency $w$. In the light of these observations on the uniform state, we naturally

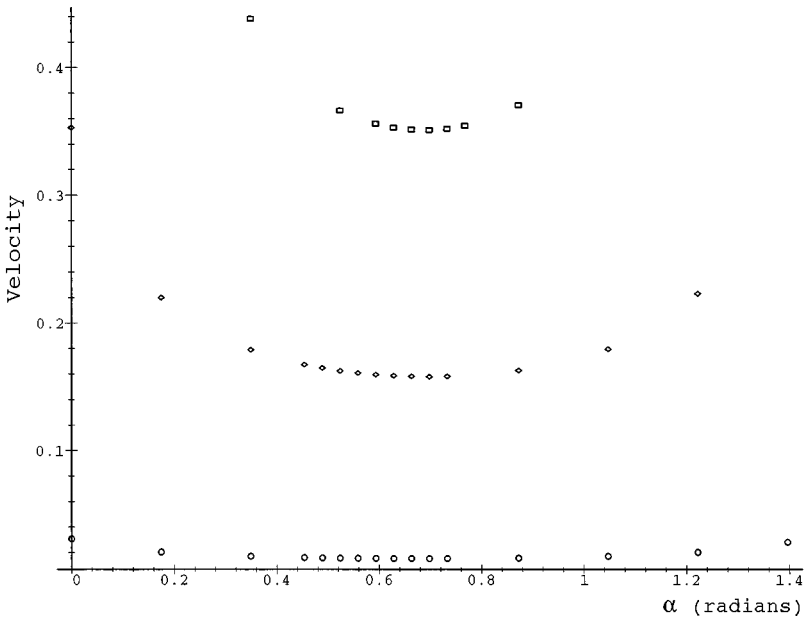


FIG. 13. Velocity of a $2\pi$ kink as a function of the tilt $\alpha$ in geometry of Fig. 1(a). Here $a=1$, and $b=0$, and, $\omega_0=0.01$ (○), 0.1 (◇), and 0.2 (□).

expect the structure and dynamics of kinks to be time dependent. We have not been able to determine quantitatively the general characteristics of this state. We address ourselves to the behavior of a kink in the phase-oscillating regime $w=0$ and the phase-slipping regime $w\neq 0$. We shall discuss how sensitively the dynamics of a $2\pi$ kink depend upon the parameters of the geometry. Also, we shall quantitatively estimate the direction of kink propagation.

We find in the phase-oscillating regime, the structure and width of the $2\pi$ kink fluctuates with the period $T$ of the oscillating field. This can be considered as a consequence of the fact that the uniform state follows the field oscillating with a time period $T$ about a direction fixed relative to the field.

We now consider the phase-slipping regime. For certain values of $w$, there again exists a fluctuating kink structure but with a periodicity equal to $nT$. To visualize the dynamics of a $2\pi$ kink, we have employed the scheme of following the ''marked'' states at $u_m=[u(\eta)-u(-\infty)]=\pi/2$, $\pi$, and $3\pi/2$ . The width of the soliton is taken to be the distance between $u_m=\pi/2$ and $u_m=3\pi/2$ states. In Figs. 15(a) and 15(b), we show the features of a kink which correspond to values of $(m,n)=(1,2)$ and $(m,n)=(1,1)$, respectively. The different periodicities are clearly evident. In the numerical technique of the method of lines, we find that the accuracy with which the system of ordinary differential equations are integrated forward in time should be much greater in the case where $w\neq 0$ than the case where $w=0$.

For those values of $w$ at which there does not exist a well-defined periodicity, we find that the behavior of the kink does not depend on the fraction $m/n$ but rather on $n$. We have seen an oscillatory behavior for $(m,n)=(5,1)$, but an aperiodic behavior for $(m,n)=(13,10)$. The dynamics of such $2\pi$ kinks with an aperiodic behavior is similar to its dynamics in the asynchronous regime. In this case we observe that after $\tau=nT$, the structure does not return to its original state. If observed over long-time scales, the kink width increases gradually.

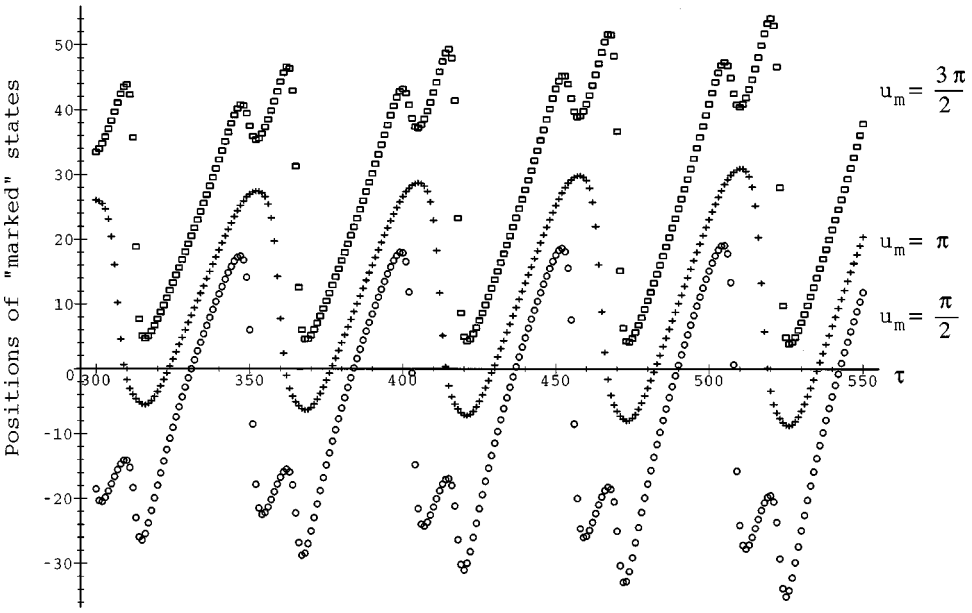


FIG. 14. A $2\pi$ kink in geometry of Fig. 1(a) in the asynchronous regime. Time evolution of the ''marked'' states, $u_m=\pi/2$ (○), $\pi$ (+), and $3\pi/2$ (□). In the asynchronous regime a $2\pi$ kink with an unique structure is not permitted. It is seen that the kink has a translational motion superimposed on oscillatory motion. Here $a=1$, $b=0$, $\omega_0=0.2$, $\alpha=10°$, and $\theta=\pi/6$ rad.

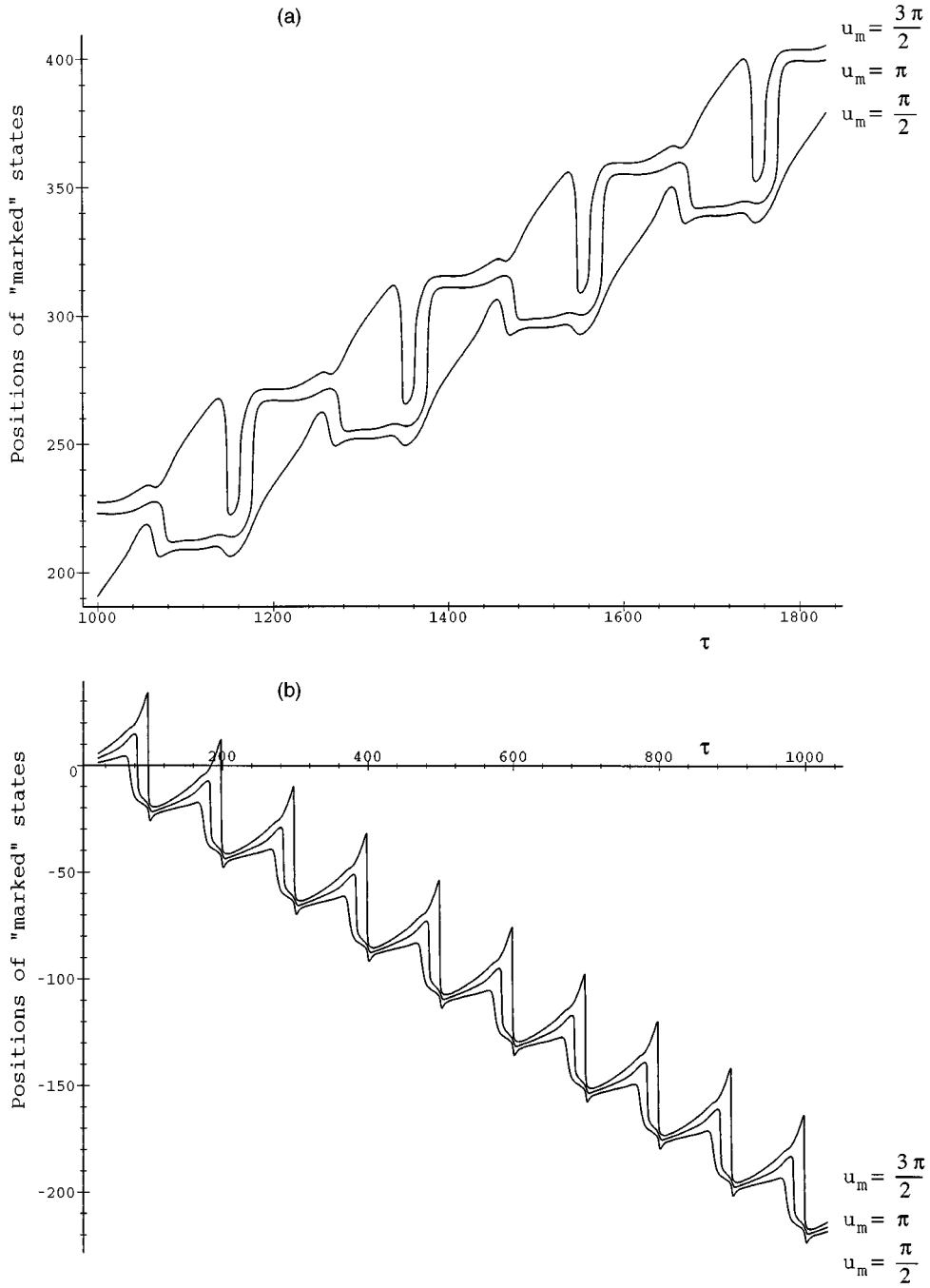


FIG. 15. A $2\pi$ kink in geometry of Fig. 1(a). The time evolution of the ''marked'' states $u_m=\pi/2$, $\pi$, and $3\pi/2$ in an oscillating field. Here $a=1$, $b=0.5$, $\gamma_0=2\pi/100$, and $\omega_0=0.1$. (a) $\alpha=10°$, $(m,n)=(1,2)$. The state $\phi=0$ expands at the expense of the state $\phi=\pi$. The time period of the oscillating kink is $\tau=200$, i.e., $2T$. (b) $\alpha=20°$, $(m,n)=(1,1)$. The state $\phi=\pi$ expands at the expense of the state $\phi=0$. The time period of the oscillating kink is $\tau=100$, i.e., $T$.

The last question we would like to address is whether we can determine the direction of propagation of a $2\pi$ kink in the cases where there exists a periodic behavior. From the cases we considered, we find that the answer is not as simple as in the synchronous regime in a nonoscillating field. Compare Figs. 15(a) and 15(b) for which $\alpha=10°$ and $\alpha=20°$, respectively, and for which the only parameter varied is the tilt. We do see that the direction of kink drift in Fig. 15(a) is opposite to what is indicated in Fig. 15(b). We can determine the direction of drift in a simpler way for these cases where the kink fluctuates periodically.

A kink moves because its internal structure breaks the spatial symmetry of the potential energy. In the frame of reference of the rotating field, the azimuthal angle $u$ that the uniform director makes with the field decides the direction of propagation. When $\alpha=0$ (or $\alpha\neq 0$), the direction of propagation reverses as $u$ changes by $\pi/2$ (or $\pi$). This can be easily understood. The orientation of the base states determine the region within the kink that is at a higher potential energy. Once we obtain this, we know that the states of lower potential energy would then propagate into the higher potential states. When there is phase slipping, there will be periods of nearly constant motion and periods of stick-slip during which the structure, direction of propagation, and velocity changes rapidly. We define an average azimuthal angle $u_{\rm av}$ of the uniform state by

$$u_{\rm av}=\frac{\int_{\tau_0}^{\tau_0+nT}u(\tau)d\tau}{nT}. \tag{16}$$

Here $n$ still defines the number of cycles of the oscillating field after which the uniform state reaches an equivalent state

as defined by $w$. Even if there is phase slipping, if the kink fluctuates periodically, we find that when $\alpha=0$ (or $\alpha\neq 0$), the direction of kink propagation reverses as $u_{\rm av}$ changes by $\pi/2$ (or $\pi$). For the cases considered in Figs. 15(a) and 15(b), we obtain $u_{\rm av}/2\pi=-0.5135$ and $u_{\rm av}/2\pi=-0.3707$, respectively. Hence, by solving the ordinary differential equation (5), we obtain $u_{\rm av}$, from which the direction of drift can be obtained.

#### *5. Lattice of kinks*

In an oscillating field, a knowledge of the dynamics of a single kink is sufficient to predict the behavior of a lattice of kinks. Equivalent states behave identically. In cases where the single kink is a uniformly traveling front, or where its structure pulsates, we find that the lattice also behaves the same way. In the asymptotic limit, the distance between equivalent states is a constant, while the distance between nonequivalent states vary periodically with time. In the asynchronous regime or in the equivalent phase slipping, the behavior of the lattice is nothing but that of a single kink with equivalent states behaving identically.

## IV. CONCLUSION

In a nonrotating oscillating field tilted with respect to the layer normal of a Sm*C* liquid crystal, we show that the structure, width, and instantaneous velocity of a $\pi$ kink fluctuates with the period of the oscillating field. The dependence of the average velocity of the kink on the tilt angle of the field indicates that there is velocity selection, and that the system is possibly choosing between families of solutions. When a nonoscillating field is rotated in a plane normal to the smectic layers, a $\pi$ kink has a nonzero drift velocity which depends upon the sense of rotation. In this geometry it is also found that a $2\pi$ kink could be in a bound oscillating state or split into oppositely drifting $\pi$ kinks depending upon the direction of the rotation of the field. In an oscllating field rotating about the layer normal, we find that the motion of the kinks can be predicted to a large extent by studying the dynamics of the uniform state. In a nonoscillating field, in the asynchronous regime, the kink fluctuates aperiodically with a slow migration. In an oscillating field, kink motion is basically decided by a phase-slip frequency which varies discontinuously with the frequency of rotation of the field. Its dynamics has both periodic and aperiodic features, being very sensitive to the parameters of the geometry.


[1] D. G. Aronson and H. F. Weinberger, Adv. Math. **30**, 33 (1978).
[2] M. C. Cross and P. C. Hohenberg, Rev. Mod. Phys. **65**, 851 (1993), and references therein.
[3] G. Dee and J. S. Langer, Phys. Rev. Lett. **50**, 383 (1983).
[4] E. Ben-Jacob *et al.*, Physica D **14**, 348 (1985).
[5] Wim van Sarloos, Phys. Rev. A **37**, 211 (1988).
[6] Wim van Sarloos, Phys. Rev. A **39**, 6367 (1989).
[7] G. C. Paquette *et al.*, Phys. Rev. Lett. **72**, 76 (1994).
[8] G. C. Paquette and Y. Oono, Phys. Rev. E **49**, 2368 (1994).
[9] R. D. Benguira and M. C. Depassier, Phys. Rev. Lett. **73**, 2272 (1994).
[10] A. Goriely, Phys. Rev. Lett. **75**, 2047 (1995).
[11] R. D. Benguira and M. C. Depassier, Phys. Rev. Lett. **77**, 1171 (1996).
[12] R. D. Benguira and M. C. Depassier, Phys. Rev. Lett. **77**, 2847 (1996).
[13] *Solitons in Liquid Crystals*, edited by L. Lam and J. Prost (Springer-Verlag, Berlin, 1991).
[14] Kalman B. Migler and Robert B. Meyer, Phys. Rev. Lett. **66**, 1485 (1991).
[15] Kalman B. Migler and Robert B. Meyer, Phys. Rev. E **48**, 1218 (1993).
[16] Wim van Sarloos, Martin van Hecke, and Robert Holyst, Phys. Rev. E **52**, 1773 (1995).
[17] P. Schiller, G. Pelzl, and D. Demus, Liq. Cryst. **2**, 21 (1987).
[18] I. W. Stewart, T. Carlsson, and F. M. Leslie, Ferroelectrics **148**, 41 (1993).
[19] I. W. Stewart, T. Carlsson, and F. M. Leslie, Phys. Rev. E **49**, 2130 (1994).
[20] P. G. de Gennes and J. Prost, *The Physics of Liquid Crystals* (Clarendon, Oxford, 1993).
[21] M. Büttiker and R. Landauer, Phys. Rev. A **23**, 1397 (1981).
[22] F. M. Leslie, I. W. Stewart, and M. Nakagawa, Mol. Cryst. Liq. Cryst. **198**, 443 (1991).
[23] P. Jung, J. G. Kissner, and P. Hänggi, Phys. Rev. Lett. **76**, 3436 (1996).
[24] J. Armero *et al.*, Phys. Rev. Lett. **76**, 3045 (1996).